Lawrence Berkeley National Laboratory
LBL Publications

Title
Simulation of beam–beam interaction with crab cavities for LHC upgrade

Permalink
https://escholarship.org/uc/item/2b4593wh

Authors
Qiang, J
Paret, S
Ratti, A
et al.

Publication Date
2018-08-01

DOI
10.1016/j.nima.2018.05.055

Peer reviewed

Contents lists available at ScienceDirect

Nuclear Inst. and Methods in Physics Research, A

journal homepage: www.elsevier.com/locate/nima

Simulation of beam–beam interaction with crab cavities for LHC upgrade

J. Qiang [a,*], S. Paret [a], A. Ratti [a], J. Barranco [b], T. Pieloni [b], G. Arduini [c], X. Buffat [c], Y. Papaphilippou [c]

[a] *Lawrence Berkeley National Laboratory, Berkeley, CA, 94720, United States*
[b] *Particle Accelerator Physics Laboratory, Institute of Physics, EPF, Lausanne, Switzerland*
[c] *CERN, Geneva 23, CH-1211, Switzerland*

ARTICLE INFO

ABSTRACT

The crab cavities are a critical component in the high luminosity LHC upgrade project to compensate the luminosity loss from large crossing angle collision. However, these crab cavities will not be perfect in the real accelerator. In this paper, we studied the effects of crab cavity imperfections on colliding beam luminosity lifetime degradation for the LHC upgrade through detailed numerical simulations. Our simulation results suggest that the white noise jitter in the crab cavity RF phase and voltage rms amplitudes should be kept below a few 10^{-5} for a good luminosity lifetime, while with frequency-dependent jitter, the amplitudes should be kept below a few 10^{-4} for a good lifetime. The RF multipole errors in the current crab cavity designs are small enough and would not cause extra luminosity degradation.

1. Introduction

The Large Hardon Collider (LHC) with its 13 TeV center of mass energy is the highest energy hadron collider in the world and has made a number of important scientific discoveries since its construction. At interaction points (IPs) of the LHC, two counter moving proton beams collide with each other with a crossing angle in order to mitigate the effects of long-range beam–beam interactions. On the other hand, using a crossing angle collision results in the loss of luminosity by a geometric factor:

$$L = L_0 \frac{1}{\sqrt{1 + \tan(\theta_c/2)\sigma_z/\sigma_x}} \qquad (1)$$

where L_0 is the nominal luminosity, θ_c is the full crossing angle, σ_z is the root mean square (RMS) bunch length, σ_x is the horizontal RMS beam size. In order to compensate this geometric loss, crab cavities near the interaction region were proposed to deflect two beams before and after each collision [1]. By appropriately choosing the location of the crab cavities and the voltage of the cavities, the two colliding beams can be brought into collision with almost zero synchrotron–betatron coupling [2]. This improves the luminosity of colliders. The crab cavities have been built and tested at the KEKB collider for global compensation and showed improvement of the colliding luminosity [3].

High luminosity (HL) LHC upgrade will improve the luminosity of the current LHC operation by an order of magnitude [4]. In the HL

LHC, the beta* at the IPs can be as low as 0.15 m instead of 0.55 m in the nominal LHC design. The crossing angle in the HL LHC (used in this study) will be 590 μrad (this angle has been reduced to 500 μ rad since the first conceptual design report [5]) instead of 285 μrad in the nominal design. In order to reduce the luminosity loss from the larger crossing angle, crab cavities were proposed in the HL LHC to compensate the geometric loss from the crossing angle collision [6]. These crab cavities can be used to minimize the effective crossing angle at the IP, to maximize the length of the luminous region, and to reduce the line pile-up density in the longitudinal plane to allow easier vertex reconstruction for the experiments. At present, this critical component of the LHC upgrade project is being actively pursued.

A schematic plot of the crab cavity compensation layout for the LHC upgrade is given in Fig. 1. Here, a local compensation scheme is employed at each interaction point. A crab cavity at a location with 90 degree phase advance before the IP is used to deflect the beam transversely so that the two beams will collide head-on without a crossing angle at the IP. After collision, another crab cavity at a location of 90 degree phase advance downstream the IP is used to uncrab the beam and remove the beam tilt through the rest of the LHC.

To see how the crab cavity will help the LHC upgrade, we show in Fig. 2 the normalized luminosity with respect to the LHC design value as a function of beta function value at IP (beta*) with the crab cavity compensation from the strong–strong beam–beam simulation together

---

* Corresponding author.
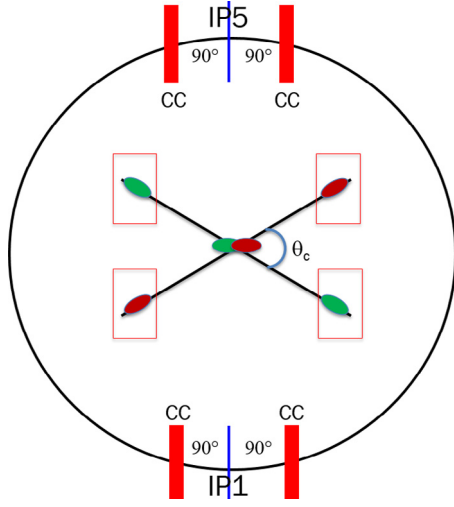 *E-mail address:* jqiang@lbl.gov (J. Qiang).

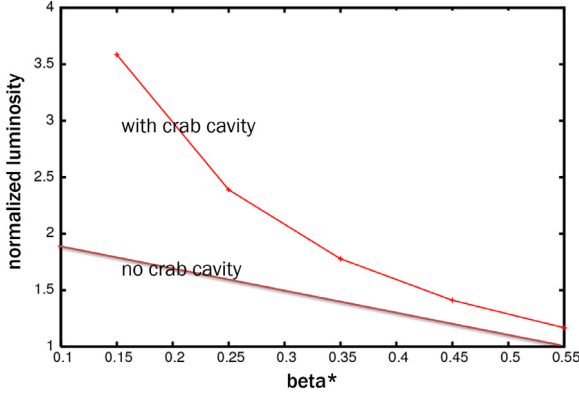**Fig. 1.** A schematic plot of the crab cavity layout for the LHC upgrade.

Fig. 2. Normalized luminosity as a function of beta* with/without crab cavity compensation.

multipole errors on colliding beam luminosity is presented in Section 5; the conclusions are drawn in Section 6.

2. Computational setup

All simulations presented in this study were done using a parallel beam–beam interaction simulation code, BeamBeam3D [8,9]. The BeamBeam3D is a 3D parallel particle-in-cell code for modeling strong–strong or strong–weak beam–beam interactions in high energy ring colliders. This code includes a self-consistent calculation of the electromagnetic forces (i.e. beam–beam forces) from two colliding beams (i.e. strong–strong modeling), a soft-Gaussian approximation of the beam–beam forces model, a linear transfer map model for beam transport between collision points, a stochastic map to treat radiation damping, quantum excitation, an arbitrary orbit separation model, a single map to account for chromaticity effects, and models of conducting wire, crab cavity, electron lens for beam–beam compensation. It can handle multiple bunches from each beam collision at multiple interaction points (IPs) with arbitrary separation and crossing angle. The parallel implementation is done using a particle-field decomposition method to achieve a good load balance. It has been applied to studies of the beam–beam effects in a number colliders such as RHIC, Tevatron, LHC, and KEK-B [10–14].

A linear transfer map is used to transport the colliding beams in LHC between interaction points. This is because in this study, we are concerned about the beam emittance growth and luminosity degradation due to the beam–beam interactions together with crab cavity imperfections in the LHC upgrade. The emittance and the luminosity are mainly affected by core particles. Without crab cavities, the dominant nonlinear effects will be the beam–beam forces. The inclusion of the crab cavity RF multipole errors is to check the potential time-dependent effects from those errors (e.g. tune modulation) on the beam emittance growth and luminosity degradation.

The fully strong–strong beam–beam model provides a self-consistent modeling of the beam–beam interaction and beam evolution. However, this method is very time consuming and also subject to numerical noise induced artificial emittance growth due to finite macroparticles used in the simulation [15]. Such a numerical emittance growth shadows the true physics driven emittance growth. In order to reduce numerically induced emittance growth, and to gain computational speed, the beam–beam interaction fields were computed assuming a Gaussian particle distribution using the bunch centroids and the RMS sizes calculated from the ensemble of macroparticles in the simulation before each collision. This assumption is justified by the fact that the initial Gaussian particle distribution does not change significantly in a short period of time under stable conditions. In the simulation, we have used one million macroparticles for each beam. The particle distribution in the longitudinal direction was divided into 8 slices. Two collisions per turn, corresponding to the interaction points (IPs) 1 and 5 in the LHC, were simulated. The crossing plane is horizontal at IP 5 (CMS experiment) and vertical at IP 1 (ATLAS experiment). Linear transfer maps, calculated using the working point tunes and beta functions, were employed to transfer the beam between collisions. The crab cavities are located at 90 degree phase advance from each IP. To model the beam transport through the crab cavity, we have assumed a thin lens approximation where the transfer map in the x–z plane for each particle i is given by

$$x_i^{n+1} = x_i^n \tag{2}$$

$$P_{xi}^{n+1} = P_{xi}^n + \frac{qV}{E} \sin(\omega z_i^n/c + \phi) \tag{3}$$

$$z_i^{n+1} = z_i^n \tag{4}$$

$$\delta E_i^{n+1} = \delta E_i^n + \frac{qV\omega}{Ec} x_i^n \cos(\omega z_i^n/c + \phi) \tag{5}$$

where P_x and P_y are transverse momenta normalized by E/c, δE is the total momentum deviation normalized by E/c, qV/E is the normalized

with a plot without compensation. It is seen that using the crab cavity does help improve the peak luminosity especially at lower beta*. For the beta* at 15 cm, the peak luminosity increases by about a factor two by using the crab cavity compensation.

The above simulation results assumed that the crab cavity parameters follow the ideal analytical model for a LHC beam with 3.5 μm normalized emittance and 7.5 cm rms bunch length. In reality, both the crab cavity RF voltage and the RF phase will not be exact as the designed values. The noise from the low-level RF control will result in fluctuations (jitters) of both the crab cavity voltage and the phase. Furthermore, the RF field distribution inside the cavity does not necessarily follow the ideal distribution. There are RF multipole fields inside the cavity besides the deflecting dipole field.

Some beam dynamics aspects of crab cavities in the LHC were reported in a previous study [7]. However, this study did not take into account of the voltage, phase, and RF multipole errors in the crab cavities. In this paper, we studied the effects of these cavity imperfections together with beam–beam interaction on colliding beam luminosity lifetime in the HL LHC upgrade through detailed numerical simulations.

The organization of this paper is as follows: After the Introduction, we describe the computational setup used in this study in Section 2; the effect of white RF noise in crab cavity on colliding beam luminosity is presented in Section 3; the effect of frequency-dependent RF noise on colliding beam luminosity is presented in Section 4; the effect of RF

Table 1
Beam parameters in the LHC benchmark and upgrade simulations.

	Benchmark LHC	HL-LHC
$N/10^{11}$	1–9	1.1–2.2
$\epsilon_n/\mu m$	4.0	2.5
β^*/m	0.5	0.15 and 0.49
σ_z/m	0.075	0.075
Q_x	64.31	62.31
Q_y	59.32	60.32
$\theta/mrad$	0	0.59
Chromaticity	0	0
f_{CC}/MHz	–	400.8
Collisions/turn	1 hor.	1 hor., 1 ver.
Feedback gain	0.02	0.05

voltage of the crab cavity, ω is the angular frequency of the crab cavity, c is the speed of light in vacuum, E is the beam energy, and ϕ is the phase of cavity. A similar transfer map near IP 1 with x replaced by y is used in the y–z plane. In order to compensate the crossing angle induced luminosity loss, the voltage of the crab cavity is chosen as:

$$V = \frac{Ec \tan(\theta_c/2)}{q\omega\sqrt{\beta^*\beta_{cc}}} \tag{6}$$

where β^* is the beta function value at the IP, β_{cc} is the beta function value at crab cavity location, and θ_c is the full crossing angle at IP. In this study, the β_{cc} is 4000 m in the HL-LHC simulations.

The RF noise errors in the crab cavity include both the relative voltage error and the phase error. The phase error $\delta\phi$ in the crab cavity causes beam transverse center offset at the interaction point as:

$$\delta x \approx \frac{c}{\omega} \tan(\theta_c/2)\delta\phi. \tag{7}$$

This error is also called the zeroth-order error. The RF phase error was studied at KEKB with crab cavities and showed potential danger to the colliding beam luminosity [16].

The RF voltage error $\frac{\delta V}{V}$ in the crab cavity results in a tilt in particle beam distribution as:

$$\delta x_i \approx \frac{\delta V}{V} \sin(\omega z_i^n/c + \phi) \tag{8}$$

This error causes effectively the transverse beam size increase and is also called the first-order error.

The emittance growth due to random offset white noise during beam–beam interaction in hadron colliders was studied analytically in Ref. [17]. As a test of our computational model, we simulated two colliding beams using the nominal LHC parameters subject to the transverse offset white noise during the collision. A list of the physical parameters used in this benchmark and the LHC upgrade simulation (in the following sections) is given in Table 1. The beam is round transversely with the same rms sizes and emittances in both horizontal and vertical directions.

The emittance growth rate was calculated from the simulation results and compared with the analytical prediction. Here, the analytical estimate of the emittance growth rate (1/hr) is given by:

$$\frac{1}{\epsilon_0}\frac{d\epsilon}{dt} = 5.389 \times 10^6 (\frac{\delta x}{\sigma_x})^2 \frac{1}{(1 + g/(2\pi\xi))^2} \tag{9}$$

where $\frac{\delta x}{\sigma_x}$ is the white noise RMS amplitude, g is the feedback gain, ξ is the beam–beam parameter. Fig. 3 shows the emittance growth rate as a function of beam–beam parameter with a random white noise RMS amplitude of 0.001 and a feedback gain factor of 0.02 from the simulation and from the above analytical model. It is seen that the simulation agrees with the analytical model quite well.

In the above test, a simple feedback model was used in the simulation by subtracting the transverse momenta of each particle quantities that are equal to the gain times the bunch centroid momenta in each dimension after each turn. A more sophisticated feedback model that includes Hilbert filter with delay was implemented in the BeamBeam3D
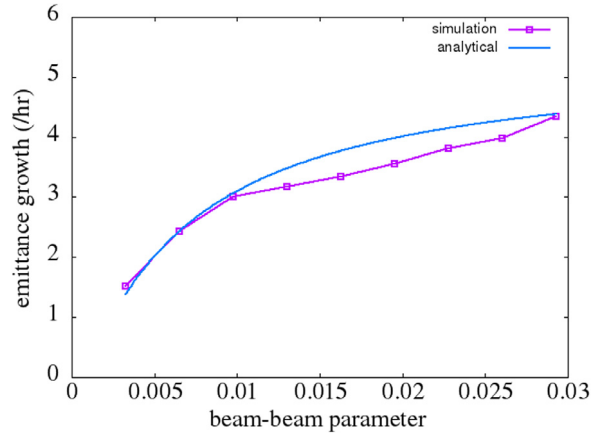

Fig. 3. Emittance growth as a function of beam–beam parameter from the simulation (purple) and from the analytical model (blue). (For interpretation of the references to color in this figure legend, the reader is referred to the web version of this article.)
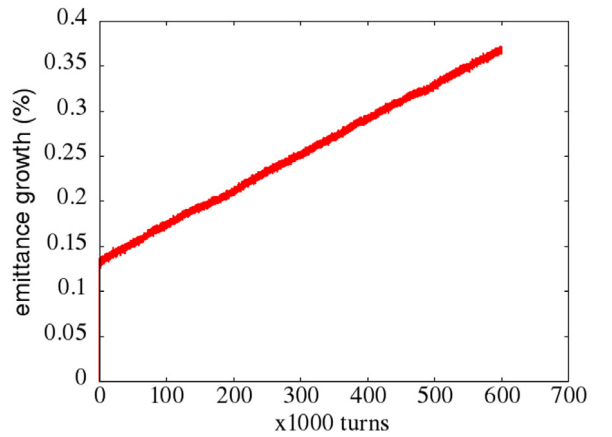

Fig. 4. Emittance growth evolution with 0.8×10^{-4} random white phase noise in HL LHC.

code and used in most of this study [18]. It turns out that the colliding beam luminosity degradation rate is not very sensitive to the details of the feedback model. An ideal feedback model that assumes the removal of the bunch centroid offset after each turn was also used in some of this study.

3. Effects of crab cavity white noise

Using the above computational model, we first studied the effects of crab cavity white noise on colliding beam luminosity degradation. The beta* used in the simulation is 0.49 m. The machine linear chromaticity is zero. The proton beam bunch intensity is 2.2×10^{11} with 2.5 μm normalized emittance. Figs. 4 and 5 show averaged emittance growth and luminosity evolutions with a random white noise in the phase of the crab cavity. Here, the white noise RMS amplitude is 0.8×10^{-4}. It is seen that emittance grows linearly as a function of time driven by the random phase noise. The initial jump of the emittance growth is due to initial charge redistribution to rematch to the lattice setting including both the crab cavities and the beam–beam effects. As the emittance growth increases, the colliding beam luminosity decreases linearly as a function of time.

In order to quantify the speed of luminosity degradation, we define a luminosity degradation rate by linearly fitting the luminosity evolution in the simulation. Fig. 6 shows the noise induced luminosity degradation
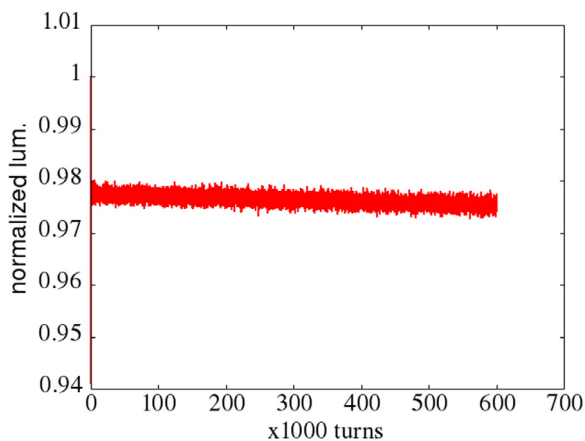
Fig. 5. Normalized luminosity evolution with 0.8×10^{-4} random white phase noise in HL LHC.
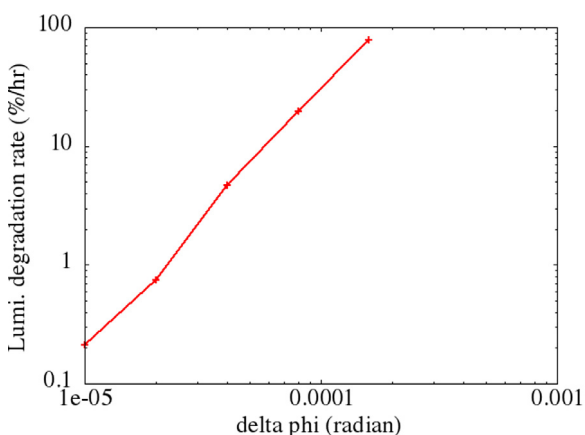

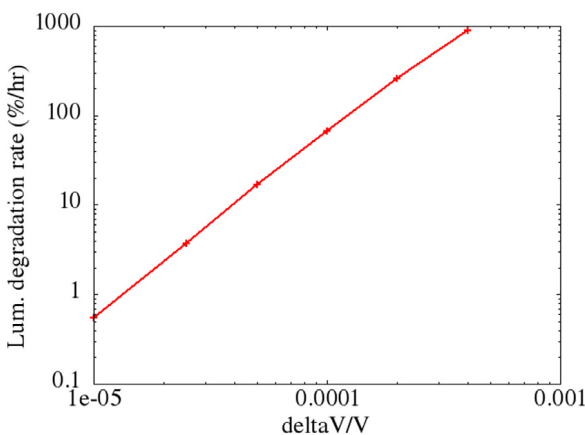**Fig. 6.** Luminosity degradation rate as a function of the crab cavity phase white noise amplitude.

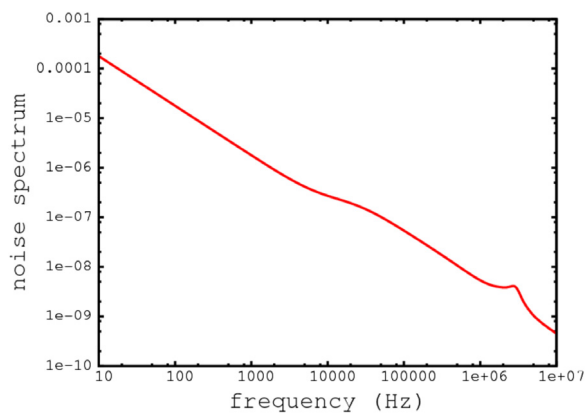**Fig. 7.** Luminosity degradation rate as a function of the amplitude of the crab cavity relative voltage white noise.

Fig. 8. Power spectrum of the crab cavity RF phase noise.

Fig. 9. Phase (red) and amplitude (green) errors of the crab cavity as a function of time. (For interpretation of the references to color in this figure legend, the reader is referred to the web version of this article.)

Fig. 7 shows the noise induced luminosity degradation rate as a function of the RMS amplitude of the crab cavity relative voltage white noise. The luminosity degradation rate grows quickly with the increase of the random voltage noise amplitude. Again, in order to keep the luminosity degradation rate below 5%/hr, the voltage noise amplitude has to be controlled below a few 10^{-5}. Similar tolerances on the crab cavity phase and voltage random white noise were also observed in Ref. [19].

4. Effects of frequency-dependent crab cavity noise

The above simulations assumed random white noise in the crab cavity RF phase and voltage. In practice, the noise inside the cavity from the low-level RF control is not a white noise but has a frequency dependency [20,21]. Fig. 8 shows the expected crab cavity phase noise power spectrum, based on the LHC low level RF noise spectrum, expected improvements, and the feedback loop bandwidth. The RMS amplitude in the time domain for this noise is 3×10^{-4}. It is clear that this phase error is not just white noise.

In this study, we assumed that the RMS phase and voltage errors follow the same power spectrum since both are related to the RF control system. Given the noise frequency spectrum, we generated the time-dependent noise data for the use in the simulation. Here, we assumed that the noise in each crab cavity is independent of each other. In order to get the phase and voltage errors in each turn, we took 256 samplings of a white noise with a random normal distribution N(0,1) per turn to reach MHz in frequency domain, and for 131,072 turns; Then we made an FFT of the random white noise data and obtained the white
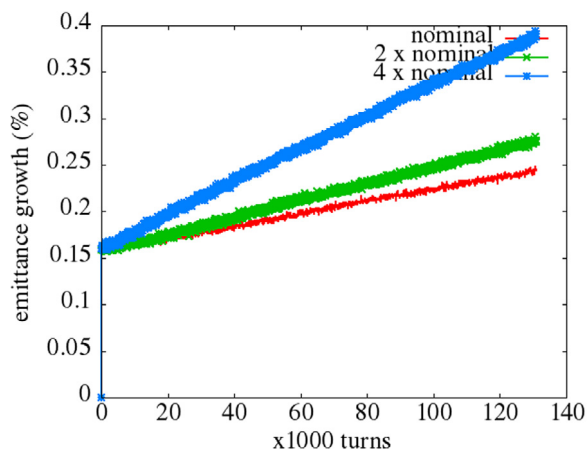
rate as a function of RMS amplitude of the random phase noise. The luminosity degradation rate grows quickly with the increase of the random phase noise amplitude. In order to keep the luminosity lifetime of 20 hours, the degradation rate needs to be controlled below 5%/hr. This suggests that the phase noise amplitude needs to be controlled below a few 10^{-5}.

Fig. 10. Emittance growth evolution with nominal, two times the nominal, and three times the nominal noise level.

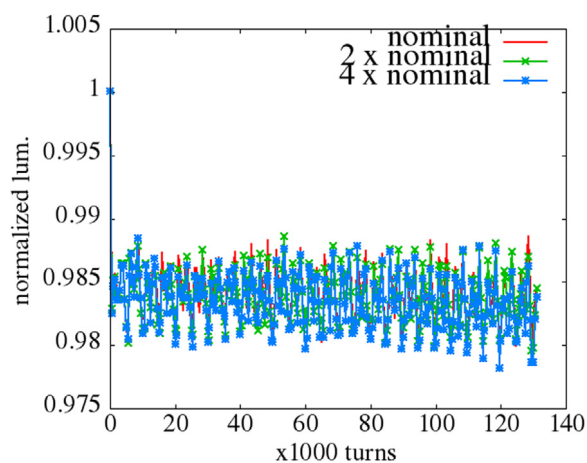**Fig. 11.** Luminosity evolution with nominal, two times the nominal, and three times the nominal noise level.

Fig. 12. Luminosity degradation rate as a function of the normalized noise amplitude using the more sophisticated feedback model (red) and the ideal feedback model (green) with 0.15 m beta*. (here 1 corresponds to nominal 3×10^{-4} RMS noise level). (For interpretation of the references to color in this figure legend, the reader is referred to the web version of this article.)

noise in frequency domain. Then we multiplied that white noise data in frequency domain with the given frequency-dependent RF noise data. Here, the original frequency-dependent RF noise data was converted from dB into regular dimensionless unit. Then we made an inverse FFT of the new noise data back to the time domain. After that we selected only one data point for every 256 data points to obtain the turn by turn noise data used in this study. We scaled the turn-dependent noise amplitude to the nominal RMS noise amplitude of 3×10^{-4}. Fig. 9 shows the time evolution of the RF phase and voltage errors. There are another 14 time-dependent error data like those in Fig. 9 for eight crab cavities used in the simulation. These noise data were read into the code during the process of simulation including total eight crab cavities (four for each beam at two IPs).

Fig. 10 shows the emittance evolution with the nominal, two times the nominal and four times the nominal noise amplitude in the simulation. Here, the nominal noise RMS amplitude level is 3×10^{-4} and we have assumed 2.2×10^{11} protons bunch intensity and 0.15 m beta* at the IPs. Both the phase noise and the voltage noise are included in the simulation with an ideal feedback model. It is seen that the RF noise from the crab cavity results in emittance growth, and this becomes worse with larger amplitude of the noise. Fig. 11 shows the luminosity evolution for these three noise amplitudes. Here, there is no intrabeam scattering effect or particle burning off in the simulation model. As the noise amplitude increases, the luminosity decreases faster. Fig. 12 shows the noise induced luminosity degradation rate as a function of the noise
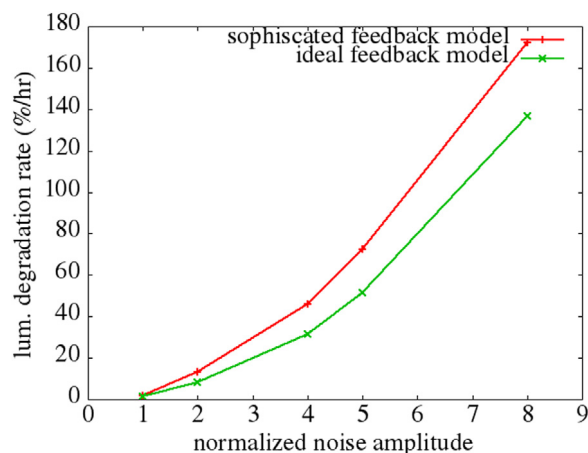
amplitude with the ideal feedback model and the more sophisticated feedback model and 0.15 m beta* at the IPs. It is seen that the luminosity degradation rate grows roughly quadratic with respect to the noise amplitude using both feedback models. The luminosity degradation rate using the ideal feedback model is somewhat smaller than that using the sophisticated feedback model with a gain of 0.05. These simulation results are consistent with the theoretical model of Eq. (9). In order to keep the luminosity degradation rate below 5%/hr, one should keep the noise amplitude level below the nominal amplitude level. The beta* at the IP affects the beam size during the collision. For the 2.2×10^{11} bunch intensity, another operational setting of the beta* is 0.49 m (Note these beta* does not necessarily represent the beta* in the latest plan. The leveled beta* now is 0.64 m.). Fig. 13 shows the noise induced luminosity degradation rate as a function of the noise amplitude with the ideal feedback model and 0.49 m beta* at the IPs. With the larger beta* at IPs, the noise induced luminosity degradation rate becomes smaller. This is because the relative noise amplitude (with respect to beam transverse size) becomes smaller assuming that the lattice parameters at crab cavity location stay the same. To keep the luminosity degradation rate below 5%/hr, the RMS noise amplitude has to be kept below two to three times the nominal amplitude level.

5. Effects of crab cavity RF multipole errors

The RF fields inside the crab cavity will not be ideal but have multipole components [22,23]. In this study, we modeled the impact of the RF multipole errors (up to decapole) inside the crab cavities as thin lens kicks in addition to the original crab cavity kick. These kicks are given by:

$$
\begin{aligned}
P_{xi}^{n+1} = P_{xi}^{n} + \frac{qc}{E} \sin(\omega z_i^n/c + \phi) \times \\
[b_2 x_i + b_3(x_i^2 - y_i^2) + b_4(x_i^3 - 3x_i y_i^2) + \\
b_5(x_i^4 - 6x_i^2 y_i^2 + y_i^4)]
\end{aligned}
\tag{10}
$$

$$
\begin{aligned}
P_{yi}^{n+1} = P_{yi}^{n} - \frac{qc}{E} \sin(\omega z_i^n/c + \phi) \times \\
[b_2 y_i + b_3 2 x_i y_i + b_4(3x_i^2 y_i - y_i^3) + \\
b_5(4x_i^3 y_i - 4x_i y_i^3)]
\end{aligned}
\tag{11}
$$

$$
\begin{aligned}
\delta E_i^{n+1} = \delta E_i^{n} + \frac{qc}{E} \cos(\omega z_i^n/c + \phi)\frac{\omega}{c} \times \\
[b_2(x_i^2 - y_i^2)/2 + b_3(x_i^3 - 3x_i y_i^2)/3 +
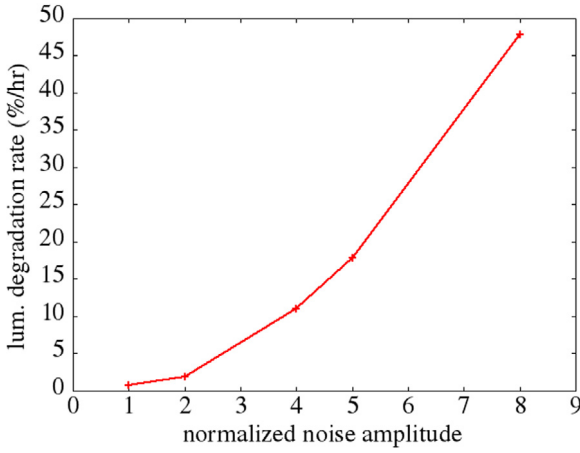\end{aligned}
$$

Fig. 13. Luminosity degradation rate as a function of the normalized noise amplitude with 0.49 m beta* (here 1 corresponds to nominal 3×10^{-4} RMS noise level).
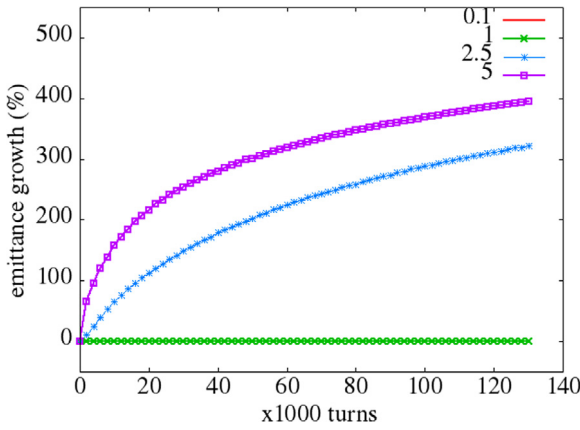

Fig. 15. The luminosity evolution with several RF quadrupole errors.

Fig. 14. The emittance growth evolution with several RF quadrupole errors.

Fig. 16. The emittance growth evolution with several RF sextupole errors.

$$b_4(x_i^4 - 6x_i^2 y_i^2 + y_i^4)/4 +$$
$$b_5(x_i^5 - 10x_i^3 y_i^2 - 3x_i y_i^4)/5] \tag{12}$$

where b_2, b_3, b_4, and b_5 denote the integrated amplitudes of quadrupole, sextupole, octupole, and decapole errors inside the crab cavity. The quadrupole error will cause tune shift, the sextupole error will change the linear chromaticity of the machine, and the octupole will cause amplitude dependent tune shift [23]. Figs. 14 and 15 show the emittance growth evolution and the luminosity evolution for several (0.1, 1, 2.5 and 5 T) quadrupole component errors inside the crab cavity. Here, we have used 2.2×10^{11} bunch intensity with 0.49 m beta*, zero chromaticity and nominal noise level. It is seen that when the integrated quadrupole error reaches 2.5 T, there are significantly nonlinear emittance growth and significant luminosity degradation. Below the 1 T, there are little emittance growth and luminosity degradation. In all current versions of the crab cavity design for the LHC upgrade, this error component is below 0.2 T [23] and would not cause extra luminosity degradation.

Figs. 16 and 17 show the emittance growth evolution and the luminosity evolution for several (10, 160, 1280 and 2560 T/m) sextupole errors inside the crab cavity. There are little emittance growth and luminosity degradation up to 160 T/m the sextupole error in the cavity. Beyond 1280 T/m sextupole error, there are significant emittance growth and luminosity degradation. The integrated sextupole error in the current crab cavity design is below 10 T/m [23], which would not cause noticeable luminosity degradation.
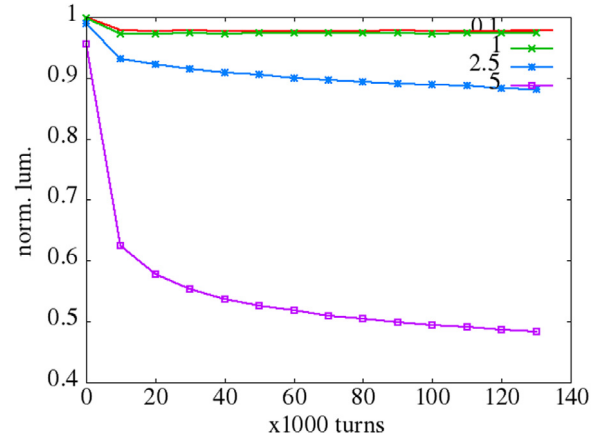

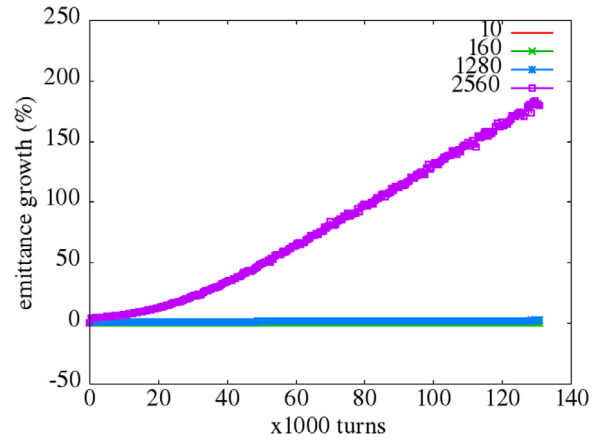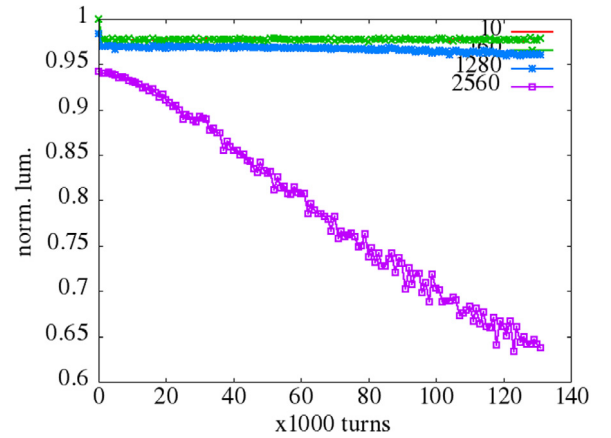**Fig. 17.** The luminosity evolution with several RF sextupole errors.

Figs. 18 and 19 show the luminosity evolution with several octupole errors (10, 100, 200, 500 T/m/m) and decapole errors (500, 1000, 2000, 4000 T/m/m/m). It is seen that up to 500 T/m/m octupole error and 4000 T/m/m/m decapole error, there is no noticeable luminosity degradation. The octupole error in the current design of the crab cavity is below 100 T/m/m and the decapole error is below 3000 T/m/m/ [23], which would not cause any extra luminosity degradation.
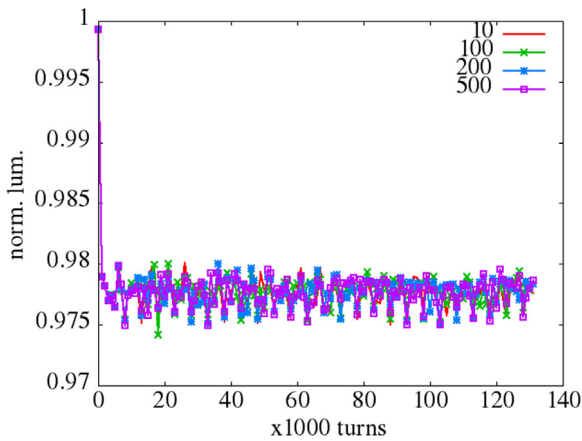
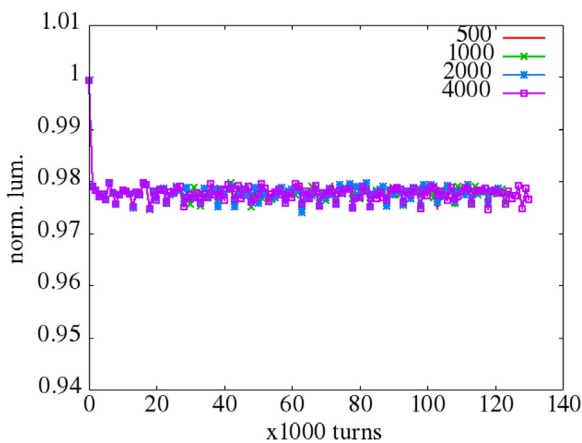**Fig. 18.** The luminosity evolution with several RF octupole errors.

Fig. 19. The luminosity evolution with several RF decapole errors.

6. Conclusions

In this paper, we reported on detailed numerical simulations of the beam–beam interaction with crab cavities for the LHC upgrade. This study suggests that the imperfections in the crab cavities (e.g. phase and voltage noise jitters) could result in significant colliding beam luminosity degradation. If the phase and voltage jitters were random white noise, the RMS amplitudes of these noises had to be kept below a few 10^{-5} to have a good luminosity lifetime. In the real RF cavities, these noises would not be random white noise but have frequency dependence. Using a noise power spectrum, based on the LHC low level RF noise spectrum, expected improvements, and the feed-back loop bandwidth, our simulation results suggest that the amplitudes of these jitters should be kept below a few 10^{-4} for a good luminosity lifetime.

We also studied the effects of multipole errors in crab cavity field distribution. The simulation results suggest that the RF multipole errors inside the current crab cavity designs are small enough and would not cause extra luminosity degradation.

References

[1] R.B. Palmer, Stanford Linear Accelerator Center Report No. SLAC-PUB-4707, 1988 (unpublished).
[2] K. Oide, K. Yokoya, Phys. Rev. A40 (1989) 315.
[3] T. Abe, et al., Prog. Theor. Exp. Phys. 2013 (2013) 03A0010.
[4] O.S. Bruning, F. Zimmermann, Proc. of IPAC2012, New Orleans, MOPPC005.
[5] G. Apollinari, I. Bejar Alonso, O. Bruning, M. Lamont, L. Rossi (Eds.), HL-LHC Preliminary Design Report, CERN-2015-004, 2015.
[6] R. Calaga, et al., Proc. of PAC07, Albuquerque, TUPAS089.
[7] Y. Sun, et al., Phys. Rev. ST Accel. Beams 20 (2009) 101002.
[8] J. Qiang, M. Furman, R. Ryne, Phys. Rev. ST Accel. Beams 5 (2002) 104402.
[9] J. Qiang, M.A. Furman, R.D. Ryne, J. Comput. Phys. 198 (2004) 278.
[10] J. Qiang, M. Furman, R.D. Ryne, W. Fischer, T. Sen, M. Xiao, Proc. Beam-Beam03, May 19–23, Montauk, NY, 2003, p. 278.
[11] K. Ohmi, M. Tawada, Y. Cai, S. Kamada, K. Oide, J. Qiang, Phys. Rev. Lett. 92 (2004) 214801.
[12] J. Qiang, Proc. PAC2005, Knoxville, Tennessee, May 16–20, 2005, p. 535.
[13] J. Qiang, M.A. Furman, R.D. Ryne, W. Fischer, K. Ohmi, Nucl. Instrum. Methods Phys. Res. A558 (2006) 351.
[14] J. Qiang, S. Paret, T. Pieloni, K. Ohmi, Strong-strong beam-beam simulation of bunch length splitting at the LHC, in: Proc. of IPAC, 2015, p. 2210.
[15] S. Paret, J. Qiang, Proc. IPAC2013, Shanghai, China, 2013, p. 1700.
[16] K. Ohmi, et al., Phys. Rev. ST Accel. Beams 14 (2011) 111003.
[17] Y. Alexahin, Nucl. Instrum. Methods Phys. Res. A391 (1996) 73.
[18] S. Paret, J. Qiang, Proc. IPAC2012, New Orleans, Louisiana, USA, 2012, p. 1374.
[19] K. Ohmi, in: W. Herr, G. Papotti (Eds.), Proc. of ICFA Mini-Workshop on Beam-Beam Effects in Hadron Colliders, 2014, p. 69.
[20] P. Baudrenghien, T. Mastoridis, Phys. Rev. Accel. Beams 18 (2015) 101001.
[21] T. Mastoridis, P. Baudrenghien, A. Butterworth, J. Molendijk, C. Rivetta, J.D. Fox, Phys. Rev. ST Accel. Beams 14 (2011) 092802.
[22] D.R. Brett, R.B. Appleby, R. De Maria, J. Barranco García, R. Tomás García, B. Hall, G. Burt, Phys. Rev. ST Accel. Beams 17 (2014) 104001.
[23] J. Barranco García, R. De Maria, A. Grudiev, R. Tomás Garcí a, R.B. Appleby, D.R. Brett, Phys. Rev. Accel. Beams 19 (2016) 101003.